Set membership state estimation for discrete-time linear systems with binary sensor measurements[☆]

Marco Casini, Andrea Garulli [*], Antonio Vicino

Dipartimento di ingegneria dell'Informazione e Scienze Matematiche, Università di Siena, Via Roma 56, 53100 Siena, Italy

A B S T R A C T

This paper addresses the problem of state estimation for discrete-time linear systems, based on measurements provided by an output binary sensor. The problem is formulated and solved in a set theoretic framework. Two algorithms are devised for recursively computing outer approximations of the set of state vectors compatible with the information provided by the binary sensor. This allows one to obtain a nominal state estimate and to characterize the associated uncertainty. The procedures can be tuned to suitably trade off the quality of set approximations and the required computational load. An input design technique based on the computed feasible state sets, which is aimed at promoting uncertainty reduction, is provided. The case of time-varying sensor threshold is also considered and a strategy for selecting online the value of the threshold is formulated. All the proposed methods are validated in simulations on two numerical examples.

© 2023 The Author(s). Published by Elsevier Ltd. This is an open access article under the CC BY license (http://creativecommons.org/licenses/by/4.0/).

1. Introduction

Binary and quantized sensors are employed in a number of different engineering contexts. In particular, binary or threshold sensors find application in chemical processes, communication channels, automotive systems, traffic control, presence sensing and many others, mainly due to their relatively low cost and simplicity of use. Clearly, the amount of information provided by such sensors is quite limited, thus calling for tailored estimation techniques and algorithms.

In the last two decades, a large body of research has been devoted to system identification based on binary or quantized measurements, see e.g. Bottegal, Hjalmarsson, and Pillonetto (2017), Casini, Garulli, and Vicino (2011, 2012), Clinet and Juillard (2010), Guo and Zhao (2013), Leong, Weyer, and Nair (2020), Pouliquen, Pigeon, Gehan, and Goudjil (2020) and Wang, Zhang, and Yin (2003) for specific contributions and the book (Wang, Yin, Zhang, & Zhao, 2010) for an overview on the subject. On the other hand, relatively less attention has been dedicated to the problem of state estimation in the presence of binary sensor measurements. In Wang, Li, Yin, Guo, and Xu (2011) and Wang, Xu, and Yin (2008), continuous-time linear systems are considered. It is shown that the problem is equivalent to state estimation under irregularly sampled output measurements. In fact, every time the output signal crosses the sensor threshold, a new measurement becomes available. Observability, observer design and convergence properties have been studied, assuming stochastic output noise models.

The problem is significantly different in the discrete-time setting. In such a case, at each time instant the information provided by the sensor measurement just says if the output signal is above or below the sensor threshold. This results in a *deterministic* uncertainty associated to each measurement, which is present even if the sensor is noiseless. The discrete-time state estimation problem in the presence of binary sensors has been studied in various contexts, including distributed target tracking in wireless sensor networks (see, e.g., Ribeiro, Giannakis, and Roumeliotis (2006) and Teng, Snoussi, and Richard (2010)), security of cyber–physical systems (Song, Wang, Wang, Alsaadi, & Shan, 2021) and nonlinear systems (Hu, Chen, Zhang, & Yu, 2022). These works usually model the disturbances affecting the systems as stochastic processes and propose state estimation techniques based on probabilistic uncertainty description, such as Kalman or particle filtering. A different approach is taken in Battistelli, Chisci, and Gherardini (2017), where linear discrete-time systems affected by unknown-but-bounded (UBB) disturbances are considered. A moving horizon state estimator is devised, whose stability is proven under suitable observability assumptions, and a recursive bound on the state estimation error is provided. An alternative way to deal with the deterministic error associated to the binary

measurements is proposed in Zhang, Chen, and Yu (2020). It should be also pointed out that in the discrete-time setting the choice of a suitable input signal may be crucial to ensure that the output crosses the sensor threshold a sufficient number of times, thus making it possible to gather sufficient information on the state evolution.

A key observation when dealing with binary sensors is that the uncertainty associated to the measurements provides a set-valued information on the state vector to be estimated. In fact, the state vectors compatible with a single binary measurement define a half-space in the state domain. If also process disturbances and measurement noise are described using set-theoretic models, like in the UBB setting, the state estimation problem can be naturally cast in a *set membership* estimation framework (Milanese & Vicino, 1991). Set membership state estimation has a long history, now spanning more than five decades, starting from the pioneering works (Bertsekas & Rhodes, 1971; Schweppe, 1968). Since then, a number of alternative approaches have been proposed (see, e.g., Alamo, Bravo, and Camacho (2005), Althoff and Rath (2021), Chisci, Garulli, and Zappa (1996), Combastel (2015), Durieu, Walter, and Polyak (2001), El Ghaoui and Calafiore (2001), Gollamudi, Nagaraj, Kapoor, and Huang (1996), Kieffer, Jaulin, and Walter (2002), Scott, Raimondo, Marseglia, and Braatz (2016), Wang, Wang, Puig, and Cembrano (2019) and references therein), which have been employed in a wide variety of application domains. The main advantage of such techniques is that they allow to compute, at each time instant, the set of all the state vectors compatible with the entire sequence of measurements collected up to that time, thus providing a full geometric characterization of the uncertainty associated to the state estimate. However, to the best of the authors' knowledge, set membership state estimation techniques have not been considered so far in the case of binary or quantized measurements.

In this paper, the state estimation problem for linear discrete-time systems with binary sensor measurements is addressed in a set membership framework. Three main contributions are provided. First, two set membership state estimation algorithms, based on outer approximations of the exact feasible state set, are proposed. They provide guaranteed bounds on the uncertainty affecting the state estimates, by exploiting the information contained in the binary measurements. The number of past measurements to be processed is used as a tuning knob to trade off the quality of the feasible set approximations and the computational load. The second contribution is an input design technique which is aimed to promote uncertainty reduction. Finally, in the case in which the threshold of the binary sensor can be changed over time, a suitable strategy to select the threshold in order to reduce the estimation uncertainty is presented. All the proposed methods are validated in simulation, on two numerical examples.

The paper is organized as follows. Section 2 contains preliminary material on set manipulations. The set membership state estimation problem is formulated in Section 3. The two proposed set approximation techniques are presented in Section 4. Active state estimation based on input design or on the use of a variable threshold is discussed in Section 5. In Section 6, the results of numerical simulations on two case studies are presented, while some concluding remarks are reported in Section 7.

2. Preliminaries

In this section, some useful definitions and results on set manipulations are recalled. Given two sets $\mathcal{S}_1$ and $\mathcal{S}_2$, their sum is defined as

$$\mathcal{Z} = \mathcal{S}_1 + \mathcal{S}_2 = \{z : z = x + y, \ x \in \mathcal{S}_1, \ y \in \mathcal{S}_2\}.$$

When $\mathcal{S}_2$ contains a single element v, we write $\mathcal{S}_1 + v$ with the same meaning. Given a set $\mathcal{S} \subset \mathbb{R}^n$ and a matrix $A \in \mathbb{R}^{m \times n}$, the set $A\mathcal{S}$ is defined by

$$A\mathcal{S} = \{z \in \mathbb{R}^m : z = Ax, \ x \in \mathcal{S}\}.$$

We denote by $\mathcal{B}_\infty$ the unit ball in the infinity norm, i.e. $\mathcal{B}_\infty = \{x : \|x\|_\infty \leq 1\}$.

An *orthotope* (or axis aligned box) is defined by its center $c \in \mathbb{R}^n$ and semi-sides vector $d \in \mathbb{R}^n$, with $d_i \geq 0$, $i = 1, \ldots, n$, according to

$$\mathcal{O}(c, d) = \{x : x = c + \operatorname{diag}(d)\alpha, \ \|\alpha\|_\infty \leq 1\}$$

where $\operatorname{diag}(d)$ is a diagonal matrix with diagonal equal to d. The volume of the orthotope is equal to $2^n \prod_{i=1}^n d_i$.

A *parallelotope* is defined by its center $c \in \mathbb{R}^n$ and shape matrix $T \in \mathbb{R}^{n \times n}$, according to

$$\mathcal{P}(c, T) = \{x : x = c + T\alpha, \ \|\alpha\|_\infty \leq 1\}.$$

The volume of the parallelotope is equal to $2^n |\det(T)|$.

An *m-parpolygon* is defined by its center $c \in \mathbb{R}^n$ and shape matrix $T \in \mathbb{R}^{n \times m}$, according to

$$\mathcal{T}(c, T) = \{x \in \mathbb{R}^n : x = c + T\alpha, \ \|\alpha\|_\infty \leq 1\}.$$

When $m = n$, the parpolygon boils down to a parallelotope. The sum of two parpolygons is a parpolygon itself and it is given by

$$\mathcal{T}(c_1, T_1) + \mathcal{T}(c_2, T_2) = \mathcal{T}(c_1 + c_2, [T_1 \ T_2]). \tag{1}$$

A generic *polytope* $\mathcal{V}$ is defined through a set of h linear inequalities

$$\mathcal{V} = \{x \in \mathbb{R}^n : Mx \leq q\} \tag{2}$$

where $M \in \mathbb{R}^{h \times n}$ and $q \in \mathbb{R}^h$ (inequalities between vectors are always intended componentwise). Notice that a polytope can be unbounded and boils down to a half-space when $h = 1$.

The minimum orthotope containing a bounded polytope $\mathcal{V} \subset \mathbb{R}^n$ is denoted by $\bar{\mathcal{O}}[\mathcal{V}]$. Similarly, $\bar{\mathcal{P}}[\mathcal{V}]$ denotes the minimum volume parallelotope containing the polytope $\mathcal{V}$. The following result will be useful in the subsequent developments.

Proposition 1. *Given a polytope $\mathcal{V} \subset \mathbb{R}^n$ defined by (2), a vector $v \in \mathbb{R}^n$, a nonsingular matrix $A \in \mathbb{R}^{n \times n}$, a matrix $G \in \mathbb{R}^{n \times m}$, and a constant $\gamma > 0$, the following properties hold:*

$$A\mathcal{V} + v = \{x : MA^{-1}x \leq q + MA^{-1}v\} \tag{3}$$

$$A\mathcal{V} + \gamma G\mathcal{B}_\infty \subseteq \{x : MA^{-1}x \leq q + \gamma r\} \tag{4}$$

with r such that $r_i = \|(MA^{-1}G)_i\|_1$, $i = 1, \ldots, h$, and $(M)_i$ denotes the ith row of matrix M. Moreover, if $M \in \mathbb{R}^{1 \times n}$ (i.e, $\mathcal{V}$ is a half-space), (4) holds with the equality sign.

Proof. Let us first prove (3). If $x \in A\mathcal{V} + v$, one has that $x = Ay + v$, for some $y \in \mathcal{V}$. Then, using (2)

$$MA^{-1}x = MA^{-1}Ay + MA^{-1}v \leq q + MA^{-1}v.$$

Conversely, let x be such that $MA^{-1}x \leq q + MA^{-1}v$. Let $\bar{y} = A^{-1}(x - v)$. One has $M\bar{y} \leq q$ and hence $\bar{y} \in \mathcal{V}$. Moreover, $x = A\bar{y} + v$ and therefore $x \in A\mathcal{V} + v$.

Now, let us show (4). If $x \in A\mathcal{V} + \gamma G\mathcal{B}_\infty$, there exist $y \in \mathcal{V}$ and $w \in \mathcal{B}_\infty$ such that $x = Ay + \gamma Gw$. Then,

$$MA^{-1}x = MA^{-1}Ay + MA^{-1}\gamma Gw \leq q + \max_{w \in \mathcal{B}_\infty} MA^{-1}\gamma Gw$$

where the max operator has to be intended componentwise. Then, (4) follows from $\max_{w \in \mathcal{B}_\infty} v'w = \|v\|_1$, for any $v \in \mathbb{R}^n$. Finally, when $h = 1$, let x satisfy $MA^{-1}x \leq q + \gamma r$ and choose $\bar{w} \in \mathcal{B}_\infty$ such that $MA^{-1}G\bar{w} = \|MA^{-1}G\|_1 = r$. If one sets $\bar{y} = A^{-1}(x - \gamma G\bar{w})$, then $M\bar{y} = MA^{-1}x - \gamma MA^{-1}G\bar{w} \leq q + \gamma r - \gamma r = q$, i.e., $\bar{y} \in \mathcal{V}$. Hence, $x = A\bar{y} + \gamma G\bar{w} \in A\mathcal{V} + \gamma G\mathcal{B}_\infty$, and therefore (4) holds with the equality sign. $\square$

3. Problem formulation

Consider the SISO discrete-time linear system

$$x(k+1) = Ax(k) + Bu(k) + Gw(k) \tag{5}$$

$$z(k) = Cx(k) + v(k) \tag{6}$$

where $x(k) \in \mathbb{R}^n$ is the state vector, $u(k) \in \mathbb{R}$ is the input, $z(k) \in \mathbb{R}$ is the (inaccessible) output signal, $w(k) \in \mathbb{R}^d$ is the process disturbance and $v(k) \in \mathbb{R}$ is the output noise. At each time instant k, a binary sensor provides the measurement

$$y(k) = \begin{cases} 1, & \text{if } z(k) \geq \tau \\ -1, & \text{if } z(k) < \tau \end{cases} \tag{7}$$

where τ is the sensor threshold.

Assumption 1. The process disturbance $w(k)$ and the output noise $v(k)$ are UBB sequences, satisfying

$$\|w(k)\|_\infty \leq \delta_w$$

$$|v(k)| \leq \delta_v$$

for all $k \geq 0$.

Matrices A, B, C, G and bounds δ_w, δ_v can be time-varying. Hereafter, we assume they are constant to keep the notation simple, but the extension of the proposed approaches requires just minor amendments. Similarly, all the subsequent treatment can be easily extended to the case of MIMO systems.

The information provided by the binary measurement (7), along with the UBB assumption on the output noise $v(k)$, allow one to define the *feasible measurement set*, i.e., the set of states $x(k)$ which are compatible with the sensor measurement $y(k)$. This is given by

$$\mathcal{M}(k) = \left\{ x \in \mathbb{R}^n : \begin{array}{ll} Cx \geq \tau - \delta_v, & \text{if } y(k) = 1 \\ Cx < \tau + \delta_v, & \text{if } y(k) = -1 \end{array} \right\} \tag{8}$$

which, with a slight abuse of notation,[1] can be rewritten as

$$\mathcal{M}(k) = \left\{ x \in \mathbb{R}^n : y(k)(Cx - \tau) + \delta_v \geq 0 \right\}. \tag{9}$$

The set $\mathcal{M}(k)$ is a half-space in the state space, even if $\delta_v = 0$ (noiseless sensor). This motivates the adoption of a set membership approach in the state estimation problem.

It is now possible to define recursively the *feasible state set* $\Xi(k|k)$, which is the set of all the state vectors $x(k)$ which are compatible with all the binary measurements collected from the initial time $k = 0$ to the current time instant k. By letting $\Xi(0|-1)$ be the set of feasible initial states $x(0)$ (the a priori information on the initial state), one has

$$\Xi(k|k) = \Xi(k|k-1) \bigcap \mathcal{M}(k) \tag{10}$$

$$\Xi(k+1|k) = A\Xi(k|k) + Bu(k) + \delta_w G\mathcal{B}_\infty \tag{11}$$

for $k = 0, 1, 2, \ldots$. The set $\Xi(k+1|k)$ represents the set of all feasible predicted states $x(k+1)$, given the information up to time k. It can be noticed that, if $\Xi(0|-1)$ is a (bounded) polytope, then all the sets $\Xi(k|k)$ and $\Xi(k+1|k)$ are (bounded) polytopes in $\mathbb{R}^n$ (see, e.g., Chisci et al. (1996)). In order to prevent the feasible state sets from degenerating into a linear subspace, hereafter we will assume that the state transition matrix A is non-singular. This is not a restrictive assumption (in particular, when the discrete-time system has been obtained via discretization of a

continuous-time one), and anyway it can be removed at the price of more involved set representations.

The exact computation of the feasible state sets is computationally intractable even for small state dimensions. In fact, the number of vertices and facets of the polytopes $\Xi(k|k)$ grows exponentially in time. Therefore, the objective of the set membership state estimation problem is to construct suitable approximations of the feasible state sets. In particular, *outer* approximations are usually sought, so that they are guaranteed to contain all the state vectors which are compatible with the available information and hence to provide a reliable characterization of the uncertainty associated to the estimates.

4. Set approximation algorithms

In this section we present two alternative procedures for computing an outer approximation of the feasible state set. The objective is to start from a set $\mathcal{S}(0|-1) \supseteq \Xi(0|-1)$ and to recursively compute sets $\mathcal{S}(k|k)$ and $\mathcal{S}(k+1|k)$ such that they satisfy $\mathcal{S}(k|k) \supseteq \Xi(k|k)$ and $\mathcal{S}(k+1|k) \supseteq \Xi(k+1|k)$, $\forall k \geq 0$.

4.1. Block parallelotopic state estimator

The first algorithm is adapted from the recursive parallelotopic bounding techniques proposed in Chisci, Garulli, Vicino, and Zappa (1998) and Chisci et al. (1996). The approximating set $\mathcal{S}(k|k)$ is a parallelotope, defined as $\mathcal{P}(k|k) = \mathcal{P}(c(k|k), T(k|k))$, where $c(k|k)$ is the center and $T(k|k)$ the shape matrix. Let us assume that at time $k-1$, an approximating parallelotope $\mathcal{P}(k|k-1) \supseteq \Xi(k|k-1)$ has been computed. In order to perform the correction step (10), one needs to find a parallelotope $\mathcal{P}(k|k)$ so that

$$\mathcal{P}(k|k) \supseteq \mathcal{P}(k|k-1) \bigcap \mathcal{M}(k). \tag{12}$$

The computation of the minimum volume $\mathcal{P}(k|k)$ satisfying (12) has been solved in Vicino and Zappa (1996). However, when dealing with binary measurements, the information provided by a single feasible measurement set $\mathcal{M}(k)$ may lead to a very coarse approximation of the feasible state set $\Xi(k|k)$. Therefore, in order to reduce the conservatism, it may be beneficial to process simultaneously a block of past measurements. This has been observed also for continuous measurements, in the context of set membership parameter identification (Chisci et al., 1998). Here the problem is more involved, because past feasible measurement sets are iteratively modified by the system dynamics (5). For example, the feasible measurement set $\mathcal{M}(k-1)$ can be propagated to time k, to generate the set of feasible states $x(k)$ compatible with the measurement $y(k-1)$, which is defined as

$$\mathcal{M}(k|k-1) = A\mathcal{M}(k-1) + Bu(k-1) + \delta_w G\mathcal{B}_\infty.$$

Similarly, one can compute a h-step ahead propagation of the feasible measurement set $\mathcal{M}(k-h)$, defining the set of states $x(k)$ compatible with the measurement $y(k-h)$. By using (5) iteratively, this is given by

$$\mathcal{M}(k|k-h) = A^h \mathcal{M}(k-h) + \sum_{i=0}^{h-1} A^{h-1-i}Bu(k-h+i)$$

$$+ \delta_w \sum_{i=0}^{h-1} A^{h-1-i}G\mathcal{B}_\infty. \tag{13}$$

It is worth stressing that, being $\Xi(k-h|k-h) \subseteq \mathcal{M}(k-h)$ by (10), one also has $\Xi(k|k) \subseteq \mathcal{M}(k|k-h)$. Therefore, the propagated measurement sets $\mathcal{M}(k|k-h)$, for $h = 1, 2, \ldots$, do not provide any useful information when computing the exact feasible sets according to the recursion (10)–(11). Conversely, when adopting

---

[1] In (9) the strict inequality is replaced by a nonstrict one in the case $y(k) = -1$. This does not affect the development, as the condition $z(k) = \tau$ is clearly singular.

a recursive approximating procedure, such sets may be useful to further reduce the current approximated feasible sets. Motivated by this idea, let us introduce the following characterization of the propagated measurement set $\mathcal{M}(k|k-h)$.

Lemma 1. *Let the feasible measurement set at time $k-h$ be given by*

$$\mathcal{M}(k-h) = \{x \in \mathbb{R}^n : m(k-h)x \le q(k-h)\},$$

with $m(k-h) = -y(k-h)C$ and $q(k-h) = \delta_v - \tau y(k-h)$. Then, for any $h \ge 1$ the h-step ahead propagated measurement set is given by

$$\mathcal{M}(k|k-h) = \{x : m(k-h)A^{-h}x \le q(k-h)$$
$$+m(k-h)\sum_{i=0}^{h-1} A^{-(i+1)}Bu(k-h+i)$$
$$+\delta_w \sum_{i=0}^{h-1} \|m(k-h)A^{-(i+1)}G\|_1\}. \tag{14}$$

Proof. By applying properties (3)–(4) to (13) with $\mathcal{V} = \mathcal{M}(k-h)$, and noticing that $\mathcal{M}(k-h)$ is a half-space, the result easily follows. $\square$

Let us adopt the notation $\mathcal{M}(k|k) = \mathcal{M}(k)$ and set $\mathcal{M}(k|k-h) = \mathbb{R}^n$ for $h > k$. Then, following the above discussion, the correction update (10) can be approximated by the block-correction step

$$\mathcal{P}(k|k) = \bar{\mathcal{P}} \left[\mathcal{P}(k|k-1) \bigcap_{h=0}^{q_p-1} \mathcal{M}(k|k-h) \right] \tag{15}$$

where q_p is a tuning parameter that can be used to trade off accuracy of the uncertainty estimate and computational load. The computation of $\mathcal{P}(k|k)$ in (15) boils down to find the minimum parallelotope containing the intersection of a parallelotope and q_p half-spaces. To this aim, the procedure proposed in Chisci et al. (1998) can be employed.

As far as the prediction step (11) is concerned, one can obtain a parallelotopic outer bound of $\Xi(k+1|k)$ by computing

$$\mathcal{P}(k+1|k) = \bar{\mathcal{P}}\left[A\mathcal{P}(k|k) + Bu(k) + \delta_w G\mathcal{B}_\infty\right]. \tag{16}$$

Being $\mathcal{P}(k|k) = \mathcal{P}(c(k|k), T(k|k))$, using (1) it is easy to see that

$$\mathcal{P}(k|k) + Bu(k) + \delta_w G\mathcal{B}_\infty = \mathcal{T}(Ac(k|k) + Bu(k), [AT(k|k) \ \ \delta_w G])$$

which is an $(n+d)$-parpolygon. Hence, the computation of the right hand side in (16) amounts to find the minimum volume parallelotope containing a parpolygon. Several approximate solutions can be found in the literature (see, e.g., Combastel (2015) and Scott et al. (2016)). The optimal solution is derived next. Let n, m be integers, such that $n \le m$. Let $\mathcal{I}_n^m$ denote the set of tuples of n integers that can be extracted from $\{1, 2, \ldots, m\}$. Given a matrix $T \in \mathbb{R}^{n \times m}$, denote by $T^{(\kappa)}$, $\kappa \in \mathcal{I}_n^m$, the matrix obtained by selecting from matrix T the n columns whose indexes belong to the tuple κ. Hereafter, only full rank matrices $T^{(\kappa)}$ are considered.[2] Let $P^{(\kappa)} = [T^{(\kappa)}]^{-1}$ and denote by $p_i^{(\kappa)}$, $i = 1, \ldots, n$, the rows of $P^{(\kappa)}$. The next result provides the minimum volume parallelotope containing a parpolygon.

Theorem 1. *Let $\mathcal{T}(c, T)$ be a m-parpolygon, with $T \in \mathbb{R}^{n \times m}$, $m > n$, and $T = [t_1 \ t_2 \ \ldots t_m]$ is full rank. Then,*

$$\bar{\mathcal{P}}[\mathcal{T}(c, T)] = \mathcal{P}(c, \bar{T}^*)$$

where

$$\bar{T}^* = T^{(\kappa^*)} \cdot diag(q^*)$$

with

$$q_i^* = \sum_{j=1}^{m} |p_i^{(\kappa^*)} t_j|, \quad i = 1, \ldots, n$$

and

$$\kappa^* = \arg \min_{\kappa \in \mathcal{I}_n^m} \left\{ \prod_{i=1}^{n} \sum_{j=1}^{m} |p_i^{(\kappa)} t_j| \right\} \cdot |\det T^{(\kappa)}|.$$

Proof. It is easy to see that $\mathcal{T}(c, T)$ can be written as the intersection of $\binom{m}{n-1}$ strips in $\mathbb{R}^n$. In fact, each $(n-1)$-tuple of vectors t_{i_h}, $h = 1, \ldots, n-1$, defines two opposite facets of $\mathcal{T}(c, T)$, whose hyperplanes bound the strip $|p(x-c)| \le 1$, with the row vector $p \in \mathbb{R}^n$ such that $p\, t_{i_h} = 0$, $h = 1, \ldots, n-1$. By exploiting (Vicino & Zappa, 1996), one has that the n strips of the minimum bounding parallelotope $\bar{\mathcal{P}}[\mathcal{T}(c, T)]$ must be chosen among the $\binom{m}{n-1}$ ones.

Being T full rank, there is at least one full-rank matrix $T^{(\kappa)}$. Now, for each full-rank matrix $T^{(\kappa)}$, $\kappa \in \mathcal{I}_n^m$, consider the inverse $P^{(\kappa)} = [T^{(\kappa)}]^{-1}$ and its rows $p_i^{(\kappa)}$, $i = 1, \ldots, n$. Clearly, each vector $p_i^{(\kappa)}$ is orthogonal to $n-1$ columns t_i of $T^{(\kappa)}$, and therefore it is a candidate to define one of the n strips of $\bar{\mathcal{P}}[\mathcal{T}(c, T)]$. Hence, it turns out that $\bar{\mathcal{P}}[\mathcal{T}(c, T)]$ must be selected among the parallelotopes $\mathcal{P}(c, \bar{T}^{(\kappa)})$, where $\bar{T}^{(\kappa)} = T^{(\kappa)} \cdot diag(q^{(\kappa)})$ and $q^{(\kappa)}$ is chosen so that $\mathcal{P}(c, \bar{T}^{(\kappa)}) \supseteq \mathcal{T}(c, T)$. The latter condition is satisfied by imposing that

$$\min_{q^{(\kappa)} \in \mathbb{R}^n} \max_{x \in \mathcal{T}(c,T)} \|[\bar{T}^{(\kappa)}]^{-1}(x-c)\|_\infty = 1,$$

which corresponds to

$$\min_{q_i^{(\kappa)}} \max_{x \in \mathcal{T}(c,T)} \left| \frac{1}{q_i^{(\kappa)}} p_i^{(\kappa)}(x-c) \right| = 1, \quad i = 1, \ldots, n,$$

thus leading to $q_i^{(\kappa)} = \sum_{j=1}^{m} |p_i^{(\kappa)} t_j| = 1$, for $i = 1, \ldots, n$. Finally, among all the parallelotopes $\mathcal{P}(c, \bar{T}^{(\kappa)})$ one has to select the one with minimum volume. Being the volume proportional to $|\det \bar{T}^{(\kappa)}|$, one has to find

$$\begin{aligned}
\kappa^* &= \arg \min_{\kappa \in \mathcal{I}_n^m} |\det \bar{T}^{(\kappa)}| \\
&= \arg \min_{\kappa \in \mathcal{I}_n^m} \left\{ \prod_{i=1}^{n} q_i^{(\kappa)} \right\} \cdot |\det T^{(\kappa)}| \\
&= \arg \min_{\kappa \in \mathcal{I}_n^m} \left\{ \prod_{i=1}^{n} \sum_{j=1}^{m} |p_i^{(\kappa)} t_j| \right\} \cdot |\det T^{(\kappa)}|
\end{aligned}$$

which concludes the proof. $\square$

The overall Block Parallelotopic State Estimation (BPSE) procedure is summarized in Algorithm 1. An example of one iteration of the procedure, in a case with $n = 2$ and $q_p = 2$, is depicted in Fig. 1. The following result states that the BPSE procedure is guaranteed to provide an outer approximation of the true feasible state set at every time k.

Theorem 2. *Let $\mathcal{P}(0|-1) \supseteq \Xi(0|-1)$. Then, the sequence of parallelotopes $\mathcal{P}(k|k)$, $\mathcal{P}(k+1|k)$, $k = 0, 1, \ldots$, computed according to the BPSE procedure in Algorithm 1, satisfies the inclusions*

$$\mathcal{P}(k|k) \supseteq \Xi(k|k) \tag{17}$$

$$\mathcal{P}(k+1|k) \supseteq \Xi(k+1|k) \tag{18}$$

for all $k = 0, 1, \ldots$.

---

[2] Rank-deficient matrices $T^{(\kappa)}$ correspond to unbounded parallelotopes, which clearly are not candidates for the minimum volume one.
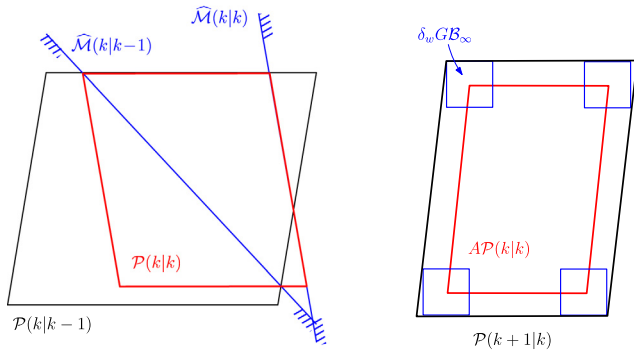
Fig. 1. Example of one iteration of the BPSE procedure, for a case with $n = 2$ and $q_p = 2$. Left: correction step (15); right: prediction step (16).

Algorithm 1 Block Parallelotopic State Estimator (BPSE)

1: Input: model A, B, C, G, δ_w, δ_v; input–output data $u(k)$, $y(k)$; number of measurements q_p to be processed at each time instant.
2: Initialize: parallelotope $\mathcal{P}(0|-1) \supseteq \varXi(0|-1)$.
3: **for** $k = 0, 1, \ldots, N$ **do**
4:     *Correction Step*
5:     **for** $h = 1, \ldots, \min\{q_p, k\}$ **do**
6:         Compute $\mathcal{M}(k|k - h)$ in (14)
7:     **end for**
8:     Compute $\mathcal{P}(k|k)$ according to (15)
9:     *Prediction Step*
10:    Compute $\mathcal{P}(k + 1|k)$ according to (16)
11: **end for**

Proof. The result can be proven by induction. For $k = 0$, one has $\mathcal{P}(0|-1) \supseteq \varXi(0|-1)$ by assumption. Then, according to (15), $\mathcal{P}(0|0) = \bar{\mathcal{P}}\left[\mathcal{P}(0|-1) \bigcap \mathcal{M}(0)\right] \supseteq \varXi(0|-1) \bigcap \mathcal{M}(0) = \varXi(0|0)$.

For a generic k, let $\mathcal{P}(k|k - 1) \supseteq \varXi(k|k - 1)$. By using (15), Lemma 1 and (10), one gets

$$
\mathcal{P}(k|k) = \bar{\mathcal{P}}\left[\mathcal{P}(k|k - 1) \bigcap_{h=0}^{q_p - 1} \mathcal{M}(k|k - h)\right]
$$
$$
\supseteq \left\{\varXi(k|k - 1) \bigcap \mathcal{M}(k) \bigcap_{h=1}^{q_p - 1} \mathcal{M}(k|k - h)\right\} = \varXi(k|k) \tag{19}
$$

where the last equality stems from $\varXi(k|k) \subseteq \mathcal{M}(k|k - h)$, for $h \geq 1$. Finally, by exploiting the set inclusion (19), together with (11) and (16), one has

$$
\mathcal{P}(k + 1|k) = \bar{\mathcal{P}}\left[A\mathcal{P}(k|k) + Bu(k) + \delta_w G\mathcal{B}_\infty\right]
$$
$$
\supseteq \{A\varXi(k|k) + Bu(k) + \delta_w G\mathcal{B}_\infty\} = \varXi(k + 1|k)
$$

which proves (18). □

4.2. Block orthotopic state estimator

In the second algorithm proposed hereafter, the approximating sets $\mathcal{S}$ are orthotopes. The main difference with the parallelotopic approach is that the shape of the approximating region is now fixed and defined by a diagonal matrix (i.e., $T = \text{diag}(d)$). Clearly, one possibility is to replicate exactly the same recursive approximating scheme proposed in Section 4.1. However, this would require to solve $4n$ linear programs (LPs) at each time iteration: $2n$ for computing the corrected orthotope $\mathcal{O}(k|k)$ and $2n$ for the predicted one $\mathcal{O}(k + 1|k)$. A possible alternative to reduce

the computational load consists in replacing the computation of the predicted orthotope $\mathcal{O}(k + 1|k)$ with that of a suitable parallelotope. One option is to use the same approach based on Theorem 1 adopted for the BPSE procedure. A computationally cheaper solution is explained next.

Let an orthotope $\mathcal{O}(k|k) = \mathcal{O}(c(k|k), d(k|k))$, with center $c(k|k)$ and semi-sides vector $d(k|k)$, be given and assume that $\mathcal{O}(k|k) \supseteq \varXi(k|k)$. This means that all feasible states $x(k)$ must satisfy the constraints

$$
\begin{bmatrix} I \\ -I \end{bmatrix} x(k) \leq \begin{bmatrix} c(k|k) + d(k|k) \\ -c(k|k) + d(k|k) \end{bmatrix}. \tag{20}
$$

The next result provides an outer approximation of the predicted feasible set $\varXi(k + 1|k)$.

Lemma 2. *Let $\varXi(k|k) \subseteq \mathcal{O}(k|k) = \mathcal{O}(c(k|k), d(k|k))$. Then, the parallelotope*

$$
\widehat{\mathcal{P}}(k + 1|k) = \mathcal{P}(Ac(k|k) + Bu(k), AD) \tag{21}
$$

where $D = \text{diag}(\delta_w a + d(k|k))$, with $a \in \mathbb{R}^n$ such that $a_i = \|(A^{-1}G)_i\|_1$ for $i = 1, \ldots, n$, satisfies

$$
\widehat{\mathcal{P}}(k + 1|k) \supseteq \varXi(k + 1|k).
$$

Proof. From (11), one has

$$
\varXi(k + 1|k) \subseteq A\mathcal{O}(k|k) + Bu(k) + \delta_w G\mathcal{B}_\infty.
$$

By applying properties (3)–(4) with $\mathcal{V}$ given by (20), one gets

$$
A\mathcal{O}(k|k) + Bu(k) + \delta_w G\mathcal{B}_\infty \subseteq
$$
$$
\left\{ x(k + 1) : \begin{bmatrix} I \\ -I \end{bmatrix} A^{-1}x(k + 1) \leq \begin{bmatrix} c(k|k) + d(k|k) \\ -c(k|k) + d(k|k) \end{bmatrix} \right.
$$
$$
\left. + \begin{bmatrix} I \\ -I \end{bmatrix} A^{-1}Bu(k) + \delta_w \begin{bmatrix} a \\ a \end{bmatrix} \right\} \tag{22}
$$

where $a_i = \|(A^{-1}G)_i\|_1$, $i = 1, \ldots, n$. The constraints in the left hand side of (22) can be rewritten as

$$
-d(k|k) - \delta_w a \leq A^{-1}(x(k + 1) - Ac(k|k) - Bu(k)) \leq d(k|k) + \delta_w a
$$

which are equivalent to the parallelotopic constraint $x(k + 1) \in \mathcal{P}(Ac(k|k) + Bu(k), AD)$. □

In the correction step, the same block processing approach illustrated in Section 4.1 is adopted. Hence, one can compute the approximating orthotope at time k as

$$
\mathcal{O}(k|k) = \bar{\mathcal{O}}\left[\widehat{\mathcal{P}}(k|k - 1) \bigcap_{h=0}^{q_o - 1} \mathcal{M}(k|k - h)\right] \tag{23}
$$

with $\mathcal{M}(k|k - h)$ as in (14) and $\widehat{\mathcal{P}}(k|k - 1)$ given by (21) at time k. This requires to solve $2n$ LPs (i.e., 2 LPs for each dimension of the orthotope).

The overall Block Orthotopic State Estimation (BOSE) procedure is summarized in Algorithm 2. The bounding property of the BOSE procedure is established by the next result.

Theorem 3. *Let $\mathcal{O}(0|-1) \supseteq \varXi(0|-1)$. Then, the sequence of orthotopes $\mathcal{O}(k|k)$, $\mathcal{O}(k + 1|k)$, $k = 0, 1, \ldots$, computed according to the BOSE procedure in Algorithm 2, satisfies the inclusions*

$$
\mathcal{O}(k|k) \supseteq \varXi(k|k)
$$
$$
\mathcal{O}(k + 1|k) \supseteq \varXi(k + 1|k)
$$

for all $k = 0, 1, \ldots.$

Proof. The proof follows the same lines of that of Theorem 2, by exploiting Lemma 2 and (23). □

Algorithm 2 Block Orthotopic State Estimator (BOSE)

1: Input: model A, B, C, G, δ_w, δ_v; input–output data $u(k)$, $y(k)$; number of measurements q_o to be processed at each time instant.
2: Initialize: parallelotope $\widehat{\mathcal{P}}(0|-1) \supseteq \varXi(0|-1)$.
3: **for** $k = 0, 1, \ldots, N$ **do**
4:     *Correction Step*
5:     **for** $h = 1, \ldots, \min\{q_o, k\}$ **do**
6:         Compute $\mathcal{M}(k|k-h)$ in (14)
7:     **end for**
8:     Compute $\mathcal{O}(k|k)$ according to (23)
9:     *Prediction Step*
10:     Compute $\widehat{\mathcal{P}}(k+1|k)$ according to (21)
11: **end for**

Remark 1. Besides the two procedures proposed in this section, other similar approaches can be devised by exploiting alternative set approximations techniques proposed in the literature. For example, one can adapt set membership recursive state bounding algorithms based on ellipsoids (Durieu et al., 2001; El Ghaoui & Calafiore, 2001; Gollamudi et al., 1996), interval analysis (Kieffer et al., 2002), zonotopes (Alamo et al., 2005; Combastel, 2015; Scott et al., 2016; Wang et al., 2019) and others. The main focus of this paper is not on the choice of the most effective set approximation technique, rather on showing that set membership estimation is a viable approach to tackle state estimation based on binary sensor measurements.

4.3. Computational load

In order to compare the proposed procedures from a computational viewpoint, we analyze the prediction and correction steps separately.

In the BPSE procedure, the correction step is performed by computing (15) through the approach proposed in Chisci et al. (1998). This requires a number of operations in the order of $O\left(\max\left\{\binom{n+q_p}{n+1}n, n^2\right\}\right)$. Clearly, only relatively small values of q_p are feasible. This parameter can be used as a tuning knob to trade off accuracy of the approximation and computational burden. As it will be apparent from the numerical tests in Section 6, small values of q_p are typically sufficient to obtain a good approximation of the true feasible state set.

In the prediction step, BPSE adopts the result in Theorem 1 to compute (16). This requires to perform $O(n^3)$ operations for each n-tuple in the set $\mathcal{I}_n^m$, thus leading to a complexity of the order $O\left(\binom{n+d}{n}n^3\right)$. Such a load is affordable when either n or d are small. In particular, when $d = 1$ it boils down to computing n scalar products, as detailed in Chisci et al. (1996). An option for reducing the computational burden, possibly at the price of a more conservative approximation, is to sequentially compute the minimum parallelotope bounding the sum of the current parallelotope and the segment $\mathcal{T}(0, \delta_w g_i)$, for $i = 1, \ldots, d$, where g_i denotes the ith column of G. Another alternative is to compute a suboptimal parallelotopic approximation, by using the same idea as in Lemma 2. Notice that these relaxations do not significantly affect the quality of the approximation when δ_w is much smaller than the size of the current feasible set. From the above discussion, one can conclude that the main computational burden associated to the BPSE procedure is due to the correction step and can be modulated by suitably choosing q_p.

As far as the BOSE procedure is concerned, the correction step is performed by computing (23), which requires the solution of

$2n$ LPs with n variables and $2n + q_o$ constraints. Similarly to q_p for BPSE, the parameter q_o can be used to increase the quality of the approximation of the feasible set, at the price of a higher computational burden. Notice however that in this case even values of q_o much larger than n may be feasible (see the examples in Section 6). The prediction step boils down to the computation of the parallelotope $\widehat{\mathcal{P}}(k+1|k)$ in (21), whose effort is negligible with respect to that of the correction step.

Summing up, the computational burden of the proposed procedures depends on the tuning parameters q_p and q_o, which in turn affect the quality of the feasible set approximations. It is worth stressing that this is the main difference with respect to using the BPSE or BOSE procedure for state estimation with continuous measurements. In fact, in the latter case, one may obtain a good quality of the feasible set approximations even with q_p or q_o equal to 1. Conversely, due to the poor information content of binary measurements, one has to increase the number of past measurements processed at every time instant to obtain tighter set approximations, which leads to a higher computational load. Nevertheless, the numerical tests in Section 6 show that the proposed procedures are computationally viable.

5. Active state estimation

In this section, two alternative ways to promote uncertainty reduction are discussed: input design and variable threshold.

5.1. Input design

In Wang et al. (2011, 2008) it has been observed that the input signal $u(t)$ plays a key role in observability and state estimation, in the presence of binary sensor measurements. Indeed, it is trivial to observe that even for a fully observable autonomous linear system, binary measurements may not provide useful information for state estimation, as shown by the following example.

Example 1. Consider system (5)–(6) with $n = 1$, $A = 1$, $B = 1$, $C = 1$, $G = 1$. Assume $\delta_w = \delta_v = 0$ and $u(k) = 0$, $\forall k \geq 0$. Let $\tau = 1$ be the threshold of the binary sensor. Then, if $x(0) < 1$, one has $\mathcal{M}(k) = \{x : x < 1\}$, $\forall k \geq 0$, while if $x(0) \geq 1$, one has $\mathcal{M}(k) = \{x : x \geq 1\}$, $\forall k \geq 0$. Hence, it turns out that $\varXi(k|k) = \varXi(0|-1) \bigcap \mathcal{M}(0)$ for all $k \geq 0$, thus meaning that all the measurements after the first one do not provide any useful information to reduce the uncertainty on the state estimates.

Example 1 suggests that one may exploit the input $u(t)$ to force the output $z(t)$ to cross the threshold of the binary sensor as many times as possible. In order to be able to achieve this objective, we make the following assumption.

Assumption 2. System (5)–(6) is fully reachable and fully observable.

Under Assumption 2, it is possible to design $u(t)$ in such a way to keep the output $z(t)$ as close as possible to the threshold τ, even in the presence of state and output disturbances. The following example motivates the set membership input design proposed in this section.

Example 2. Consider the same nominal system as in Example 1. Let $\tau = 1$, $\delta_w > 0$, $\delta_v > 0$. Let the feasible state set at the generic time k be the interval $\varXi(k|k) = [l(k), r(k)]$. The predicted feasible set turns out to be $\varXi(k+1|k) = [l(k)+u(k)-\delta_w, r(k)+u(k)+\delta_w]$. Now, let us choose the input signal $u(k)$ in such a way that the

threshold τ be the center of the interval $\Xi(k+1|k)$. This is given by

$$u(k) = \tau - \frac{l(k) + r(k)}{2} \qquad (24)$$

and leads to

$$\Xi(k+1|k) = \left[\tau - \frac{d(k)}{2} - \delta_w, \ \tau + \frac{d(k)}{2} + \delta_w\right]$$

where $d(k) = r(k) - l(k)$ is the size of the feasible interval $\Xi(k|k)$. Using (8), one can write the corrected feasible set at time $k+1$ as

$$\Xi(k+1|k+1) = [l(k+1), \ r(k+1)] =$$

$$\begin{cases} \left[\max\left\{\tau - \delta_v, \tau - \frac{d(k)}{2} - \delta_w\right\}, \ \tau + \frac{d(k)}{2} + \delta_w\right] \\ \qquad\qquad\qquad\qquad \text{if } y(k+1) = 1, \\ \left[\tau - \frac{d(k)}{2} - \delta_w, \ \min\left\{\tau + \delta_v, \tau + \frac{d(k)}{2} + \delta_w\right\}\right] \\ \qquad\qquad\qquad\qquad \text{if } y(k+1) = -1, \end{cases}$$

from which one gets

$$\begin{aligned} d(k+1) &= r(k+1) - l(k+1) \\ &= \min\left\{d(k) + 2\delta_w, \ \tfrac{1}{2}d(k) + \delta_w + \delta_v\right\}. \end{aligned} \qquad (25)$$

It easy to show that for any $d(0) > 0$, the system (25) converges to

$$\lim_{k \to +\infty} d(k) = 2(\delta_w + \delta_v).$$

In particular, in the noiseless case $\delta_w = \delta_v = 0$, the size of the feasible state interval $\Xi(k|k)$ converges asymptotically to zero. Therefore, the choice of the input signal (24) allows the binary sensor to provide indefinitely useful information for the reduction of the state uncertainty, which will converge to the minimum value compatible with the amplitude of the state and output disturbances. It is worth noticing that the selection of a random input, even if persistently exciting, would not lead to the same result. Fig. 2 reports the sizes of $\Xi(k|k)$, averaged over 1000 runs, for the noiseless scenario (top) and for the case $\delta_w = 0.01$, $\delta_v = 0.1$ (bottom). The random input signal is a white process with uniform distribution in $[-u_{\max}, \ u_{\max}]$. The initial state $x(0)$ is uniformly distributed in $\Xi(0|-1) = [-5, \ 5]$. The disturbances $w(k)$ and $v(k)$ are white processes, uniformly distributed in $[-\delta_w, \ \delta_w]$ and $[-\delta_v, \ \delta_v]$, respectively. As expected, the designed input $u(k)$ in (24) achieves the asymptotic uncertainty value $2(\delta_w + \delta_v)$, while random inputs provide much larger uncertainties.

Motivated by Example 2, a way for designing the input signal in order to promote reduction of the state estimate uncertainty is proposed next. Under Assumption 2, if $z(k)$ were available, it would be possible to design an output feedback regulator that drives the system towards the threshold value τ. In fact, one can choose

$$u(k) = F\hat{x}(k) + \frac{\tau}{g} \qquad (26)$$

where $F \in \mathbb{R}^{1 \times n}$ is such that the eigenvalues of $A + BF$ are all inside the unit circle, $g = C(I - A - BF)^{-1}B$ be the stationary gain of the closed-loop system, and $\hat{x}(k)$ is a state estimate generated by a Luenberger-type observer. In the noiseless case ($w(k) = v(k) = 0$), it is well known that the input signal (26) drives asymptotically the output $z(k)$ to τ. In particular, if one chooses the dead-beat controller, such that the eigenvalues of $A + BF$ are all equal to zero, one has that $z(k+h) = \tau, \forall h \ge n$ and $\forall x(k) \in \mathbb{R}^n$.

In the case of binary measurements, the output signal $z(k)$ is not known. As we have seen, the set-valued uncertainty associated to the measurement $y(k)$ and to the UBB disturbances $w(k)$ and $v(k)$, leads to a set membership state observer, whose
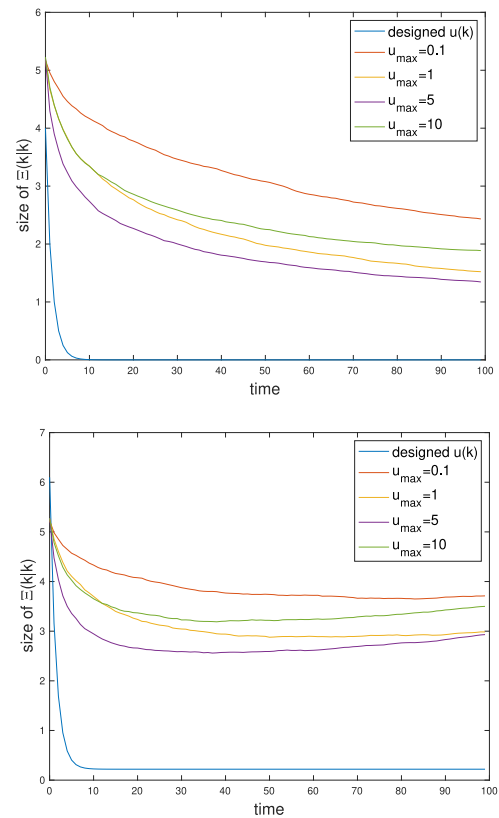
Fig. 2. Example 2. Size of feasible state sets for $u(k)$ as in (24) and for random input signals with amplitude $u_{\max}$: noiseless case (top); $\delta_w = 0.01$, $\delta_v = 0.1$ (bottom). (For interpretation of the references to color in this figure legend, the reader is referred to the web version of this article.)

estimate takes the form of the feasible state set $\Xi(k|k)$, or one of its approximations $\mathcal{S}(k|k)$ presented in Section 4. In turn, this implies that, according to the measurements collected up to time k, the signal $z(k+1)$ belongs to the *predicted output feasible set* $\mathcal{Z}(k+1|k)$, defined as

$$\mathcal{Z}(k+1|k) = C\Xi(k+1|k) + \delta_v \mathcal{B}_\infty$$
$$\subseteq \left[\min_{x \in \mathcal{S}(k+1|k)} Cx - \delta_v, \ \max_{x \in \mathcal{S}(k+1|k)} Cx + \delta_v\right]. \qquad (27)$$

In the spirit of Example 2, the idea is to choose the input $u(k)$ in such a way to drive the center of the uncertainty interval in the right hand side of (27) towards the threshold τ, so that one may expect that the binary sequence $y(k)$ will often change sign, thus resulting in more informative measurement sets $\mathcal{M}(k)$, i.e., measurement sets which provide a reduction of the feasible state set, through the intersection in (10). In particular, if the approximating set $\mathcal{S}(k|k)$ has a center of symmetry $c(k|k)$, by mimicking the input design (26), the natural choice is to set

$$u(k) = Fc(k|k) + \frac{\tau}{g}. \qquad (28)$$

In particular, one can choose $c(k|k)$ as the center of the parallelotope $\mathcal{P}(k|k)$ or the orthotope $\mathcal{O}(k|k)$, provided respectively by the BPSE or the BOSE algorithm. The following result shows that a suitable choice of F guarantees that the desired property is satisfied within a finite number of steps.

Theorem 4. *Let Assumptions 1–2 hold and assume F is the dead-beat state feedback matrix (i.e., the eigenvalues of $A + BF$ are all equal to zero). Let $\mathcal{S}(k|k)$ be a symmetric outer approximation of the feasible state set $\Xi(k|k)$, such that $\mathcal{S}(k|k) = c(k|k) + \tilde{\mathcal{S}}(k|k)$ and $x \in \tilde{\mathcal{S}}(k|k)$ if and only if $-x \in \tilde{\mathcal{S}}(k|k)$. Then, if the input signal (28)*

is chosen, one has that for all $k \geq n$, the outer approximation of the output feasible set $\mathcal{Z}(k+1|k)$ given by $C\mathcal{S}(k+1|k) + \delta_v \mathcal{B}_\infty$ is an interval centered at the threshold value τ.

Proof. Let $\tilde{x}(k) = x(k) - c(k|k)$. Clearly, $\tilde{x}(k) \in \tilde{\mathcal{S}}(k|k)$, $\forall k$. By substituting (28) into (5) one gets

$$x(k+1) = (A + BF)x(k) - BF\tilde{x}(k) + B\frac{\tau}{g} + Gw(k). \quad (29)$$

Now, by exploiting the fact that $(A + BF)^i = 0$, for $i \geq n$, from (6) and (29) one gets

$$z(k) = \sum_{i=k-n}^{k-1} C(A+BF)^{k-1-i} \left\{ B\frac{\tau}{g} - BF\tilde{x}(i) + Gw(i) \right\} + v(k) \quad (30)$$

for all $k \geq n$. Since $g = \sum_{i=0}^{n-1} C(A+BF)^i B$, (30) boils down to

$$z(k) = \tau + \sum_{i=k-n}^{k-1} C(A+BF)^{k-1-i} \left\{ -BF\tilde{x}(i) + Gw(i) \right\} + v(k). \quad (31)$$

Being $\tilde{x}(i) \in \tilde{\mathcal{S}}(i|i)$ and using Assumption 1, from (31) one gets that

$$z(k+1) \in \tau + \tilde{\mathcal{Z}}(k+1|k) \quad (32)$$

where

$$\tilde{\mathcal{Z}}(k+1|k) = \sum_{i=k-n+1}^{k} C(A+BF)^{k-i} \left\{ BF\tilde{\mathcal{S}}(i|i) + G\delta_w \mathcal{B}_\infty \right\} + \delta_v \mathcal{B}_\infty \quad (33)$$

is a symmetric interval centered in the origin, due to the symmetry of all the sets in the right hand side of (33). Therefore, $z(k+1)$ in (32) belongs to an interval centered at τ. □

If the feedback matrix F in (28) is chosen so that the closed loop system is asymptotically stable, a result similar to that of Theorem 4 can be established, but only in steady state (i.e., the center of the approximated output feasible set will approach τ asymptotically). The numerical examples in Section 6 will show that the input choice (28) is indeed effective in reducing the size of the estimated uncertainty sets.

5.2. Variable threshold

It should be remarked that, in several applications, the input signal $u(k)$ cannot be freely designed to reduce the size of the feasible state sets, for example because it is used to achieve control objectives or to optimize other performance indexes. On the other hand, in some binary sensors the value of the threshold can be adjusted by the user. Therefore, when $u(k)$ is given, one may attempt to reduce uncertainty by adopting a time-varying sensor threshold $\tau(k)$.

By following a similar reasoning as in the input design, the objective is to choose $\tau(k)$ as close as possible to the output signal $z(k)$. By exploiting again the predicted output feasible set $\mathcal{Z}(k|k-1)$, one may select $\tau(k)$ equal to the center of the interval in the right hand side of (27). For approximate feasible state sets $\mathcal{S}(k|k-1)$ with symmetry center $c(k|k-1)$, this amounts to set

$$\tau(k) = C c(k|k-1) = CAc(k-1|k-1) + CBu(k-1). \quad (34)$$

The rationale behind (34) is that the threshold is kept at the center of the approximated uncertainty interval of the output signal, thus promoting the fact that such a signal may cross the threshold itself many times, providing in turn more informative measurement uncertainty sets. This is confirmed by the numerical simulations illustrated in Section 6.

5.3. Asymptotic properties

A remarkable difference between state estimation with continuous measurements and state estimation with binary measurements lies in the asymptotic properties of the feasible state set. When continuous measurements are available, it is known that the set $\Xi(k|k)$ remains asymptotically bounded, under a detectability assumption on system (5)–(6) (see, e.g., Combastel (2015)). This can be seen as a set membership counterpart of the classic results on the asymptotic properties of the Kalman filter. However, such a property no longer holds in the case of binary measurements, even if the input signal is designed to minimize the size of the feasible state set. This is shown by the next example.

Example 3. Consider system (5)–(6) with $n = 1$, $A = a > 0$, $B = 1$, $C = 1$. Assume $\delta_w = \delta_v = 0$ (noiseless case). As in Example 2, let us denote the feasible state set at time k as $\Xi(k|k) = [l(k), r(k)]$, and its half size as $d(k) = (r(k)-l(k))/2$. We want to choose the input $u(k)$ in order to minimize the worst-case size of $\Xi(k+1|k+1)$, i.e.

$$u^*(k) = \arg \min_{u(k) \in \mathbb{R}} \sup_{x(k+1) \in \mathcal{M}(k+1)} d(k+1).$$

It is easy to verify that $u^*(k) = \tau - a\frac{l(k)+r(k)}{2}$, which corresponds to the choice (28), with $F = -a$ (dead-beat control). By setting $u(k) = u^*(k)$, from (11) one obtains $\Xi(k+1|k) = [\tau - ad(k), \tau + ad(k)]$. Therefore, being $z(k+1) = x(k+1)$, one gets

$$\Xi(k+1|k+1) = \begin{cases} [\tau, \ \tau + ad(k)], & \text{if } y(k+1) = 1, \\ [\tau - ad(k), \ \tau], & \text{if } y(k+1) = -1. \end{cases}$$

Hence, no matter the actual value of the measured binary output $y(k+1)$, the half-size of the feasible set $\Xi(k+1|k+1)$ turns out to be

$$d(k+1) = \frac{a}{2}d(k)$$

which diverges for $k \to +\infty$ when $a > 2$.

It is worth remarking that the size of the feasible set in Example 3 diverges despite the system is fully observable and the input has been designed to minimize the size of the feasible state set. Intuitively, this occurs because one binary measurement can at most halve the worst-case uncertainty and therefore the system dynamics has to at most double it in one time step, to preserve stability of the filter. Therefore, this is a fundamental limitation of state estimation with binary measurements.

On the other hand, it is easy to see that the above problem does not arise if system (5) is asymptotically stable. Indeed, even if all the measurement sets $\mathcal{M}(k)$ do not contribute to reduce uncertainty, i.e., if $\mathcal{M}(k) \supseteq \Xi(k|k-1)$, $\forall k \geq 0$, one has (for $u(k) = 0$)

$$\Xi(k+1|k+1) = A\Xi(k|k) + \delta_w G\mathcal{B}_\infty.$$

Hence, it can be shown that if A is asymptotically stable, $\Xi(k|k)$ is asymptotically included in the bounded set $\sum_{i=0}^{+\infty} A^i \delta_w G\mathcal{B}_\infty$ (see, e.g., Blanchini and Miani (2008) and Kolmanovsky and Gilbert (1998)).

6. Numerical simulations

The performance of the BPSE and BOSE algorithms are evaluated on two numerical examples.

Table 1
Double integrator. Iteration times of BPSE and BOSE over 100 runs (in milliseconds).

	mean	std
BPSE	3.04	1.42
BOSE	2.00	0.37

6.1. Double integrator

Consider the perturbed double integrator

$$x(k+1) = \begin{bmatrix} 1 & 1 \\ 0 & 1 \end{bmatrix} x(k) + \begin{bmatrix} 0 \\ 1 \end{bmatrix} u(k) + w(k)$$

$$z(k) = \begin{bmatrix} 1 & 0 \end{bmatrix} x(k) + v(k).$$

The system is simulated for $T = 200$ time instants, with $w(k)$ and $v(k)$ generated as uniformly distributed white processes satisfying Assumption 1, with $\delta_w = 0.01$ and $\delta_v = 0.05$. Being the system unstable, active state estimation via feedback design of $u(k)$ is necessary to prevent the disturbance process $w(k)$ from causing indefinite growth of the state estimation uncertainty. The input $u(k)$ has been chosen as in (28), with the dead-beat state feedback matrix $F = [-1 \ -2]$. The size of blocks of past measurements has been set to $q_p = 5$ for the BPSE algorithm and to $q_o = 20$ for the BOSE one (higher values do not lead to significant uncertainty reduction).

Fig. 3 shows the nominal estimation errors $\tilde{x}_i(k|k) = x_i(k) - c_i(k|k)$, for each state component, and the corresponding uncertainty intervals (obtained from the approximations of the feasible state sets), provided by one run of the BPSE and BOSE algorithms. Fig. 4 reports results averaged over 100 different runs of the algorithms, with initial feasible state sets equal to $\mathcal{S}(0|-1) = 5\mathcal{B}_\infty$ and initial true state $x(0)$ randomly selected within $\mathcal{S}(0|-1)$. On top, the volumes of the approximating regions are shown (blue for the BPSE algorithm, red for the BOSE one). The black line corresponds to the volume of the minimum orthotope containing the true feasible set, i.e. $\bar{\mathcal{O}}[\Xi(k|k)]$ (reported only for the sake of comparison, as the number of constraints in $\Xi(k|k)$ grows indefinitely with time). On bottom, the averaged absolute values of the nominal state estimation errors are plotted. Table 1 reports the mean and standard deviation of the times needed for a single iteration of the two approximating algorithms, over the 100 runs. All simulations have been performed in Matlab, by using IBM ILOG CPLEX for MATLAB toolbox (IBM, 2023) to solve the LPs, on an Intel Core i7-3770 at 3.40 GHz.

It can be observed that both approximation algorithms are able to successfully bound the state estimation errors, notwithstanding the persistent uncertainty injection by the disturbance process $w(k)$ and the severely limited information provided by the binary sensor. The estimate uncertainty is quite close to the minimum one, corresponding to that provided by $\bar{\mathcal{O}}[\Xi(k|k)]$, thus confirming the effectiveness of the recursive approximation procedures. It can be observed that the BOSE algorithm has a much slower transient compared to that of the BPSE, but in turn it provides slightly more accurate steady-state estimates. The reason for the slower transient of BOSE is that in the first steps only a number of predicted measurement sets $\widehat{\mathcal{M}}(k|k - h)$ much smaller than q_o are available. Notice that, the orthotopic approximation usually requires a larger number of past measurements with respect to the parallelotopic one, to achieve the same approximation quality, due to the fewer degrees of freedom in the shape matrix. On the other hand, although the two procedures show similar volumes of the approximating regions in steady state, the error in the single state component is slightly larger for BPSE, due to the fact that the approximating parallelotope tends to stretch along some directions (thus providing some relevant information about the relationship between the estimation errors in different state components).
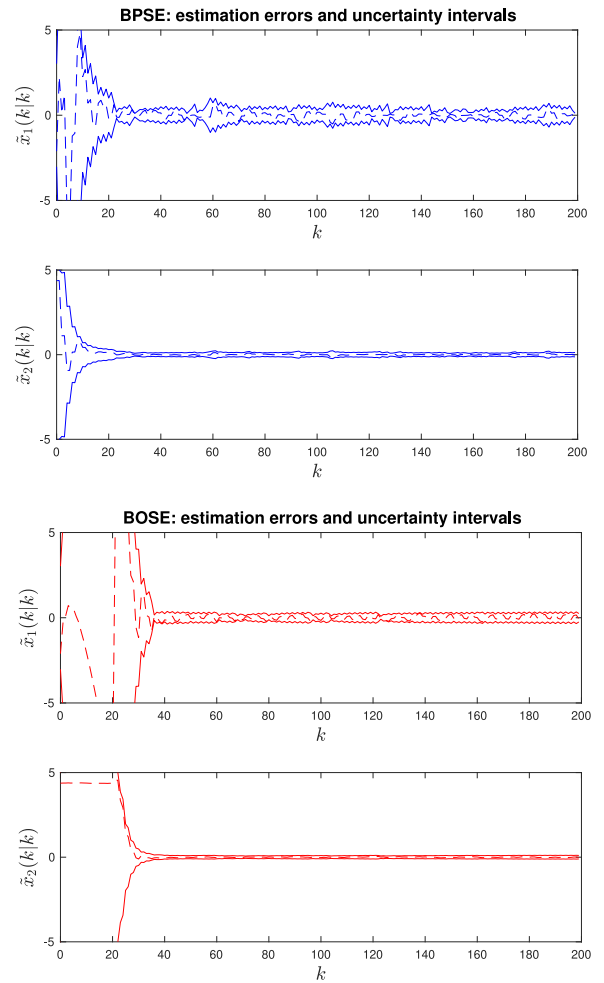
Fig. 3. Double integrator. State estimation errors (dashed) and uncertainty bounds (solid): BPSE (top, blue); BOSE (bottom, red). (For interpretation of the references to color in this figure legend, the reader is referred to the web version of this article.)

6.2. Double oscillator

Let us consider a mechanical system taken from Battistelli et al. (2017) consisting of two masses and two springs. The continuous time equations of the system are

$$\dot{x}_1(t) = x_2(t)$$
$$\dot{x}_2(t) = -\frac{k_1 + k_2}{m_1}x_1(t) + \frac{k_2}{m_1}x_3(t) + w_1(t)$$
$$\dot{x}_3(t) = x_4(t)$$
$$\dot{x}_4(t) = \frac{k_2}{m_1}x_1(t) - \frac{k_2}{m_2}x_3(t) + w_2(t)$$
$$z(t) = x_3(t) + v(t)$$

where $m_1 = m_2 = 1$ [kg] are the masses and $k_1 = k_2 = 10$ [N/m] are the stiffnesses of the springs. The disturbance process $w(t)$ represents unmodeled accelerations affecting the two masses. The system is discretized with sampling time 0.1 [s]. The discrete time process disturbance $w(k) \in \mathbb{R}^2$ and output noise $v(k)$ are generated as uniformly distributed white processes, satisfying Assumption 1.

We first consider the same experiment performed in Battistelli et al. (2017), in which the system evolves from $x(0) = [0.618, 0, 1, 0]'$, there is no process disturbance ($\delta_w = 0$), the output noise is bounded by $\delta_v = 0.05$ and the binary sensor
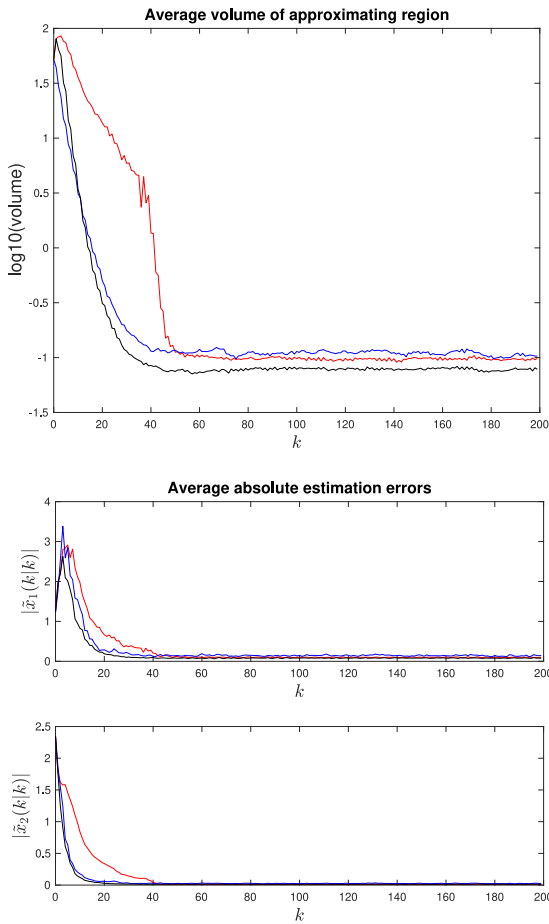
Fig. 4. Double integrator. Log-volumes of approximating regions (top) and absolute values of state estimation errors (bottom), averaged over 100 runs: BPSE (blue); BOSE (red); $\bar{\mathcal{O}}\left[\varXi(k|k)\right]$ (black). (For interpretation of the references to color in this figure legend, the reader is referred to the web version of this article.)

Fig. 5. Steady state log-volumes of approximating regions for different numbers of processed measurements q_p and q_o: BPSE (top, blue); BOSE (bottom, red).

threshold is set to $\tau = 0.5$. The selection of the number of measurements to be processed has been performed by applying the BPSE and BOSE algorithms for different values of q_p and q_o. Fig. 5 shows the volumes of the final approximating region (averaged over 100 runs) as functions of q_p and q_o. Based on these plots, the values $q_p = 5$ and $q_o = 40$ have been selected. Fig. 6 compares the true state trajectories with the nominal state estimates $c(k|k)$ provided by one run of the BPSE and BOSE algorithm. The corresponding estimation uncertainty intervals are also reported. It can be seen that, after an initial transient, both algorithms are able to effectively track the true state values. Fig. 7 shows the volumes of the approximating regions compared to that of the minimum orthotope $\bar{\mathcal{O}}\left[\varXi(k|k)\right]$ containing the exact feasible state set. Results are averaged over 100 runs with different realizations of the noise $v(k)$. Notice that the two approximating algorithms reach a steady state volume very close to that of the minimum orthotope (the volume of BPSE can be even smaller than that of the minimum orthotope, due to different shape of the parallelotope). Once again, the BOSE algorithm shows a large initial transient, due to the poor flexibility of the orthotopic approximation when very few measurements, and hence much fewer than q_o predicted measurement sets $\widehat{\mathcal{M}}(k|k-h)$, are available.

Another set of simulations has been performed by adopting a variable threshold $\tau(k)$, selected according to (34). In order to make the estimation problem more challenging, a process disturbance $w(k)$ with $\delta_w = 0.1$ has been added and the initial state

$x(0)$ has been randomly selected within $\mathcal{S}(0|-1) = 5\mathcal{B}_\infty$. Notice that this makes the problem harder, because the state trajectory is strongly affected by the choice of the initial state. Fig. 8 reports the state estimates and the corresponding uncertainties for a typical run. The volumes of the approximating regions, averaged over 100 runs with different realizations of $w(k)$, $v(k)$ and $x(0)$, are shown in Fig. 9 (top). The bottom of the same figure depicts the volumes obtained in the same setting, but with $\delta_w = 0$.

By comparing the results in Figs. 8–9 with those in Figs. 6–7, it can be observed that convergence of the nominal estimates is much faster and the steady state uncertainties are significantly smaller, thus confirming the usefulness of adapting the threshold according to the current set membership uncertainty set. In particular, it can be appreciated that the steady state values in Fig. 9 (bottom) are two orders of magnitude smaller than those in Fig. 7. Table 2 reports the mean and standard deviation of the iteration times. Comparison with Table 1 highlights that both BPSE and BOSE scale reasonably well with the number of state variables, with BOSE being slightly faster, notwithstanding the much higher number of measurements processed at each iteration. On the other hand, it is remarkable that the BPSE algorithm is able to provide a good approximation of the feasible state set by processing much less past measurements than BOSE. As a concluding observation, it is worth stressing that in all the simulations both procedures reach a steady state volume of the approximating region which is close to that of the minimum orthotope containing
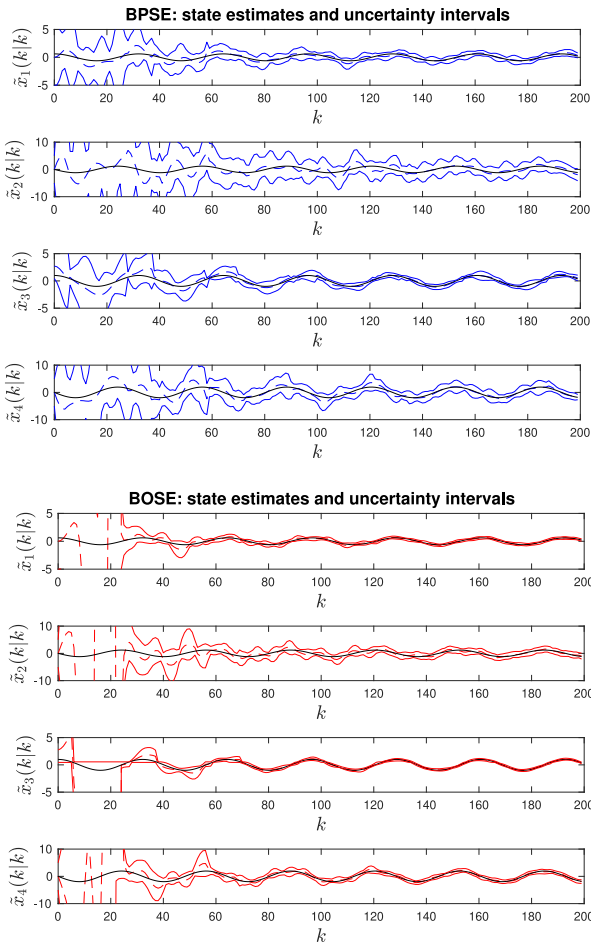
Fig. 6. Double oscillator. State estimates (dashed) and uncertainty bounds (solid), compared with true states (black): BPSE (top, blue); BOSE (bottom, red). (For interpretation of the references to color in this figure legend, the reader is referred to the web version of this article.)
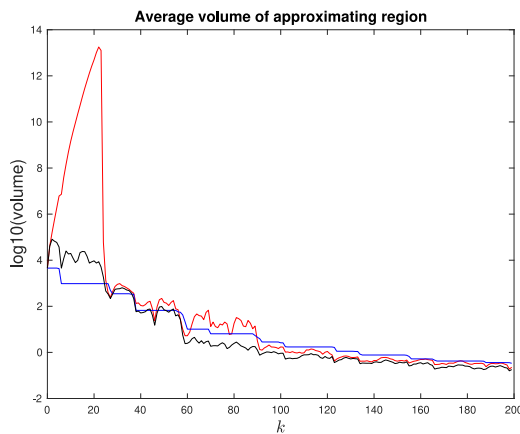
Fig. 7. Double oscillator. Log-volumes of approximating regions averaged over 100 runs: BPSE (blue); BOSE (red); $\bar{\mathcal{O}}\left[\varXi(k|k)\right]$ (black). (For interpretation of the references to color in this figure legend, the reader is referred to the web version of this article.)
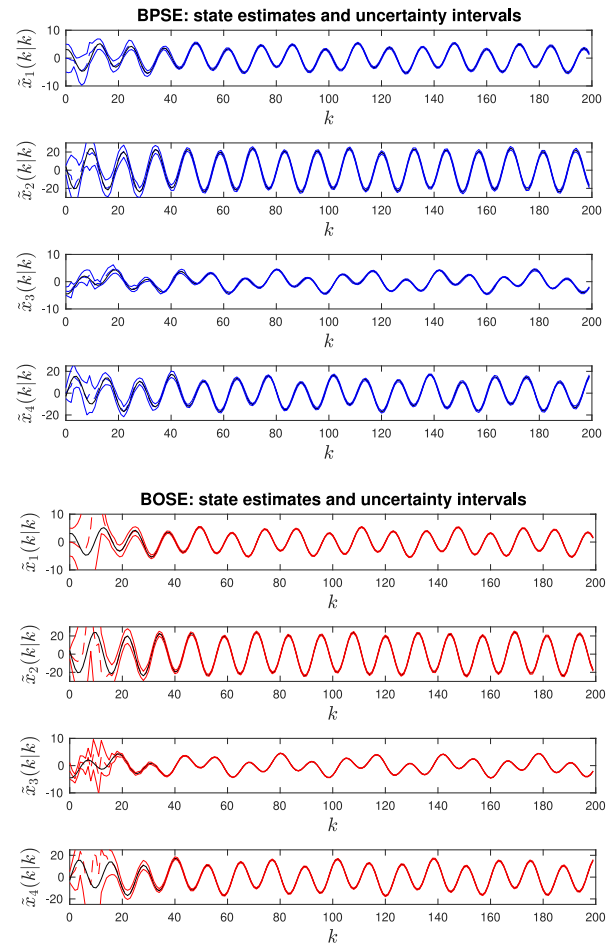
Fig. 8. Double oscillator with moving sensor threshold. State estimates (dashed) and uncertainty bounds (solid), compared with true states (black): BPSE (top); BOSE (bottom). (For interpretation of the references to color in this figure legend, the reader is referred to the web version of this article.)

Table 2
Double oscillator. Iteration times of BPSE and BOSE over 100 runs (in milliseconds).

	mean	std
BPSE	17.13	6.73
BOSE	4.00	0.45

the true feasible state set. This demonstrates that both procedures are able to provide quite tight set approximations. Therefore, the choice of the procedure to employ may be driven by the optimization of the transient behavior and by the limitations imposed by the system bandwidth.

7. Conclusions

The problem of state estimation for discrete-time linear systems has been addressed in the challenging setting of binary output measurements. Despite the limited information provided by the sensor, the proposed set-membership state estimators are able to provide both a reliable nominal estimate and a characterization of the associated uncertainty. Active estimation techniques, based either on a suitable design of the input signal or on the selection of a time-varying threshold, have proven to be effective in remarkably reducing the estimate uncertainty. The extension of the approaches proposed in this work to the case of
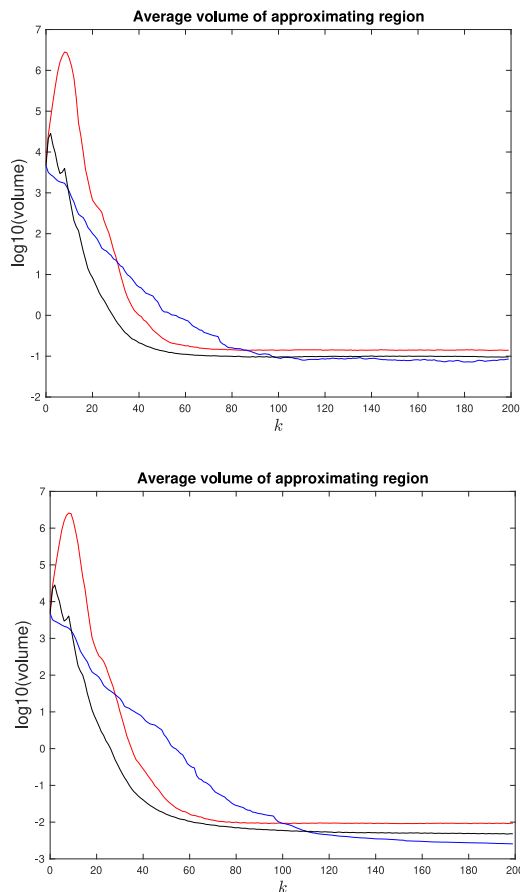
Fig. 9. Double oscillator with moving sensor threshold. Log-volumes of approximating regions averaged over 100 runs: BPSE (blue); BOSE (red); $\bar{\mathcal{O}}[\Xi(k|k)]$ (black). Top: $\delta_w = 0.01$; bottom: $\delta_w = 0$. (For interpretation of the references to color in this figure legend, the reader is referred to the web version of this article.)

quantized sensors and to state estimation for nonlinear systems, will be the subject of future research.

References

Alamo, T., Bravo, J. M., & Camacho, E. F. (2005). Guaranteed state estimation by zonotopes. *Automatica, 41*(6), 1035–1043.

Althoff, M., & Rath, J. J. (2021). Comparison of guaranteed state estimators for linear time-invariant systems. *Automatica, 130*, Article 109662.

Battistelli, G., Chisci, L., & Gherardini, S. (2017). Moving horizon estimation for discrete-time linear systems with binary sensors: algorithms and stability results. *Automatica, 85*, 374–385.

Bertsekas, D. P., & Rhodes, I. B. (1971). Recursive state estimation for a set-membership description of uncertainty. *IEEE Transactions on Automatic Control, 16*, 117–128.

Blanchini, F., & Miani, S. (2008). *Set-theoretic methods in control, Vol. 78*. Springer.

Bottegal, G., Hjalmarsson, H., & Pillonetto, G. (2017). A new kernel-based approach to system identification with quantized output data. *Automatica, 85*, 145–152.

Casini, M., Garulli, A., & Vicino, A. (2011). Input design in worst-case system identification using binary sensors. *IEEE Transactions on Automatic Control, 56*(5), 1186–1191.

Casini, M., Garulli, A., & Vicino, A. (2012). Input design in worst-case system identification with quantized measurements. *Automatica, 48*(12), 2997–3007.

Chisci, L., Garulli, A., Vicino, A., & Zappa, G. (1998). Block recursive parallelotopic bounding in set membership identification. *Automatica, 34*(1), 15–22.

Chisci, L., Garulli, A., & Zappa, G. (1996). Recursive state bounding by parallelotopes. *Automatica, 32*, 1049–1055.

Clinet, E., & Juillard, J. (2010). A weighted least-squares approach to parameter estimation problems based on binary measurements. *IEEE Transactions on Automatic Control, 55*(1), 148–152.

Combastel, C. (2015). Zonotopes and Kalman observers: Gain optimality under distinct uncertainty paradigms and robust convergence. *Automatica, 55*, 265–273.

Durieu, C., Walter, E., & Polyak, B. (2001). Multi-input multi-output ellipsoidal state bounding. *Journal of Optimization Theory and Applications, 111*(2), 273–303.

El Ghaoui, L., & Calafiore, G. (2001). Robust filtering for discrete-time systems with bounded noise and parametric uncertainty. *IEEE Transactions on Automatic Control, 46*(7), 1084–1089.

Gollamudi, S., Nagaraj, S., Kapoor, S., & Huang, Y. F. (1996). Set-membership state estimation with optimal bounding ellipsoids. In *Proceedings of the international symposium on information theory and its applications* (pp. 262–265).

Guo, J., & Zhao, Y. (2013). Recursive projection algorithm on FIR system identification with binary-valued observations. *Automatica, 49*(11), 3396–3401.

Hu, Z., Chen, B., Zhang, Y., & Yu, L. (2022). Kalman-like filter under binary sensors. *IEEE Transactions on Instrumentation and Measurement, 71*, 1–11.

IBM ILOG Cplex optimizer. Online: https://www.ibm.com/analytics/cplex-optimizer.

Kieffer, M., Jaulin, L., & Walter, E. (2002). Guaranteed recursive non-linear state bounding using interval analysis. *International Journal of Adaptive Control and Signal Processing, 16*(3), 193–218.

Kolmanovsky, I., & Gilbert, E. G. (1998). Theory and computation of disturbance invariant sets for discrete-time linear systems. *Mathematical Problems in Engineering, 4*(4), 317–367.

Leong, A. S., Weyer, E., & Nair, G. N. (2020). Identification of FIR systems with binary input and output observations. *IEEE Transactions on Automatic Control, 66*(3), 1190–1198.

Milanese, M., & Vicino, A. (1991). Estimation theory for nonlinear models and set membership uncertainty. *Automatica, 27*, 403–408.

Pouliquen, M., Pigeon, E., Gehan, O., & Goudjil, A. (2020). Identification using binary measurements for IIR systems. *IEEE Transactions on Automatic Control, 65*(2), 786–793.

Ribeiro, A., Giannakis, G. B., & Roumeliotis, S. I. (2006). SOI-KF: Distributed Kalman filtering with low-cost communications using the sign of innovations. *IEEE Transactions on Signal Processing, 54*(12), 4782–4795.

Schweppe, F. C. (1968). Recursive state estimation: unknown but bounded errors and system inputs. *IEEE Transactions on Automatic Control, 13*, 22–28.

Scott, J. K., Raimondo, D. M., Marseglia, G. R., & Braatz, R. D. (2016). Constrained zonotopes: A new tool for set-based estimation and fault detection. *Automatica, 69*, 126–136.

Song, W., Wang, Z., Wang, J., Alsaadi, F. E., & Shan, J. (2021). Secure particle filtering for cyber-physical systems with binary sensors under multiple attacks. *IEEE Systems Journal, 16*(1), 603–613.

Teng, J., Snoussi, H., & Richard, C. (2010). Decentralized variational filtering for target tracking in binary sensor networks. *IEEE Transactions on Mobile Computing, 9*(10), 1465–1477.

Vicino, A., & Zappa, G. (1996). Sequential approximation of feasible parameter sets for identification with set membership uncertainty. *IEEE Transactions on Automatic Control, 41*, 774–785.

Wang, L. Y., Li, C., Yin, G., Guo, L., & Xu, C. (2011). State observability and observers of linear-time-invariant systems under irregular-sampling and sensor limitations. *IEEE Transactions on Automatic Control, 56*(11), 2639–2654.

Wang, Y., Wang, Z., Puig, V., & Cembrano, G. (2019). Zonotopic set-membership state estimation for discrete-time descriptor LPV systems. *IEEE Transactions on Automatic Control, 64*(5), 2092–2099.

Wang, L. Y., Xu, G., & Yin, G. (2008). State reconstruction for linear time-invariant systems with binary-valued output observations. *Systems & Control Letters, 57*(11), 958–963.

Wang, L. Y., Yin, G. G., Zhang, J. F., & Zhao, Y. (2010). *System identification with quantized observations*. Springer.

Wang, L. Y., Zhang, J. F., & Yin, G. G. (2003). System identification using binary sensors. *IEEE Transactions on Automatic Control, 48*(11), 1892–1907.

Zhang, Y., Chen, B., & Yu, L. (2020). Fusion estimation under binary sensors. *Automatica, 115*, Article 108861.

Marco Casini was born in Siena, Italy, in 1973. He received the Laurea degree in information engineering and the Ph.D. in Control Systems from the University of Siena, Siena, Italy, in 1999 and 2003, respectively. In 2005, he joined the Department of Information Engineering and Mathematics of the University of Siena, where he is currently an Associate Professor. In summer 2001 he was a visiting researcher at the Laboratory for Information and Decision Systems (LIDS) at the Massachusetts Institute of Technology (MIT), Cambridge, MA. He is the author of several publications in international journals and conference proceedings. His present research interests include set-membership system identification, smart grids and optimal energy management and pursuit-evasion games.

Andrea Garulli was born in Bologna, Italy, in 1968. He received the Laurea in Electronic Engineering from the University of Firenze in 1993, and the Ph.D. in System Engineering from the University of Bologna in 1997. In 1996 he joined the University of Siena, where he is currently Professor of Control Systems. He has held positions of dean of the Faculty of Engineering and director of the Department of Information Engineering and Mathematics. He is a Fellow of the IEEE and he has been member of the Conference Editorial Board of the IEEE Control Systems Society and Associate Editor of the IEEE Transactions on Automatic Control. He currently serves as Associate Editor for Automatica. He is author of more than 200 technical publications and co-author of the book "Homogeneous Polynomial Forms for Robustness Analysis of Uncertain Systems" (Springer, 2009). His present research interests include system identification, robust estimation and control, multi-agent systems, autonomous navigation and aerospace applications.

Antonio Vicino is Professor of Control Systems at the Dept. of Information Engineering and Mathematics, University of Siena (Italy), where he covered the position of Head of the Department from 1996 to 1999 and Dean of the Engineering Faculty from 1999 to 2005. In 2000 he founded the Center for Complex Systems Studies of the University of Siena, where he covered the position of Director from 1999 to 2012. From 2016 to 2021 he was the Director of the Ph.D. Program in Information Engineering and Science at the same University. From 2019 to 2023 he covered the position of President of the Italian University Council. He is the author of more than 350 technical publications; co-author of the book "Homogeneous Polynomial Forms for Robustness Analysis of Uncertain Systems", Springer-Verlag, 2009; co-editor of several books and guest editor of several special issues on robustness in identification and control. He has worked on stability analysis of nonlinear systems, time series analysis and prediction, robust control of uncertain systems. His present interests include identification of nonlinear systems, energy systems and smart grids, systems biology and applied system modeling. He has served as Associate Editor or Associate Editor at Large for several journals like IEEE Transactions on Automatic Control, IEEE Transactions on Circuits and Systems II and Automatica. He is Fellow of the IEEE and of the IFAC.